Journal of Science and Transport Technology
Journal homepage: https://jstt.vn/index.php/en

UNIVERSITY OF TRANSPORT TECHNOLOGY

Dynamic Reliability Thresholds and Adaptive Load Management for Safety-Optimized Ageing Concrete Bridges

Yu-Gang Kim[1,2*], Chi-Myong Kim[4], Chung-Song Jo[3], Song-Jin Kim[1,5], Chol-Su Ho[1,4], Yong-Sik Ham[3], Chung-Hyok Choe[1,4], Yong-Bom Ham[1,3]
[1]School of Traffic and Transportation, Beijing Jiaotong University, Beijing, 100044, China
[2]Civil Engineering Department, Railway Design & Research Institute, Pyongyang, DPR Korea
[3]Kim Il Sung University, Pyongyang, DPR Korea
[4]Pyongyang University of Transport, DPR Korea
[5]Pyongyang University of Publishing and Printing, Pyongyang, DPR Korea

Article info
Type of article:
Original research paper

DOI:
https://doi.org/10.58845/jstt.utt.2026.en.6.1.124-142

***Corresponding author:**
Email address:
23129058@bjtu.edu.cn

Received: 29/05/2025
Received in Revised Form: 20/11/2025
Accepted: 04/12/2025

Abstract: This study presents a reliability-based framework for enhancing the durability design of ageing concrete bridges by integrating time-dependent reliability (TDR) and performance-based durability design (PBDD) principles. The proposed methodology addresses these gaps through: (1) probabilistic modeling of resistance degradation and load variations, (2) dynamic adjustment of reliability thresholds to optimize maintenance strategies, and (3) a systematic linkage between target reliability indices and operational constraints. Case studies demonstrate how real-time load management can extend service life while meeting international safety standards. The framework bridges theoretical advancements with practical applications, offering actionable insights for engineers to mitigate lifecycle costs and structural risks.

Keywords: Durability, Bridge, Performance-based design, Time-dependent reliability, Deterioration, UN SDG 9: Industry, Innovation and Infrastructure.

1. Introduction

Concrete bridges form the backbone of modern transportation networks, enabling economic growth and social connectivity [1]. However, a significant portion of this infrastructure, built in the mid-20th century, is now exceeding its intended service life [1, 2, 3]. The deteriorating state of these bridges, exacerbated by environmental attacks and steadily increasing traffic loads, poses a significant challenge to safety and serviceability [3, 4]. Catastrophic events, such as the collapse of the Morandi Bridge in Italy in August 2018 [1, 5], and recurrent failures of ageing bridges in the United States [2] serve as stark reminders of the urgent need to advance durability design paradigms.

Traditional design codes, such as those based on AASHTO or Eurocode standards, often rely on deterministic methods and static reliability indices [2, 4]. These approaches fail to adequately capture the time-variant nature of material degradation and load evolution, potentially leading to suboptimal maintenance schedules, unforeseen safety risks, and elevated lifecycle costs [2]. For instance, reinforced concrete structures are particularly susceptible to deterioration from corrosion effects, especially in critical components like Gerber saddles which are exposed to environmental actions and reduced inspection possibilities [3]. This conventional approach, primarily focused on visual inspection and damage assessment at the component level, provides qualitative insights but often lacks the predictive capacity for load-carrying capacity or system-level functionality [4].

In response to these limitations, Performance-Based Durability Design (PBDD) has emerged as a flexible framework that defines structural requirements through measurable performance criteria, allowing for more adaptable solutions [4]. Concurrently, Time-Dependent Reliability (TDR) theory provides a robust probabilistic methodology to quantify the evolution of structural safety throughout a bridge's service life [2]. These advanced methodologies aim to move beyond simple visual inspections and component-level assessments, integrating deterioration models and optimization analysis tools to ensure the long-term functioning of transportation systems [4].

Recent research continues to refine these concepts. Studies have successfully demonstrated the value of integrating field measurements with numerical simulation for accurate bridge assessment [4], while others have explored advanced materials, such as pozzolans, to enhance concrete durability in aggressive environments [3]. Despite these advancements, a critical gap remains in the practical integration of TDR and PBDD into a unified, operational framework for managing ageing bridges. Many existing approaches lack a systematic linkage between time-variant reliability thresholds and real-time, actionable operational management strategies. This is particularly relevant in light of new guidelines, such as those issued by the Italian Ministry of Infrastructure following bridge failures like the Morandi Bridge collapse, which mandate specific risk classification and management protocols [2].

To address this gap, this study proposes a novel, reliability-based framework that integrates TDR and PBDD principles for the durability design and maintenance optimization of ageing concrete bridges. The primary objectives of this research are:

To develop a probabilistic model that integrates time-dependent resistance degradation with dynamic traffic load adjustment.

To establish a systematic procedure for linking time-variant reliability indices with actionable performance limits and maintenance triggers.

To validate the proposed framework through case studies, demonstrating how real-time load management can effectively extend service life while adhering to international safety standards.

The remainder of this paper is structured as follows: Section 2 provides the theoretical background. Section 3 details the proposed integrated methodology. Section 4 presents the results and case study validation, and Section 5 concludes with key findings and recommendations for future research.

2. Theoretical Background

2.1. Time - Dependent Reliability

TDR is a probabilistic approach that considers the variation of structural performance over time. It accounts for uncertainties in material properties, environmental conditions, and loading patterns, offering a more realistic assessment of structural safety and durability compared to traditional deterministic methods [6, 7].

The concept of TDR emerged from the broader field of structural reliability, which gained prominence in the 1970s with seminal works by various researchers [7]. Early applications of TDR focused on nuclear power plants and offshore structures, where safety and durability were paramount concerns [6]. The durability of concrete structures, particularly in harsh environments, is a significant concern. Recent reviews highlight that incorporating pozzolans in concrete can significantly enhance its resistance to chloride and sulfate attacks in marine conditions, offering a sustainable approach to improving longevity [6, 8]. This material science advancement is crucial for extending the service life of concrete bridges exposed to aggressive environmental factors.

In the context of bridge engineering, TDR was first applied to assess the effects of corrosion on reinforced concrete beams [6]. Since then, advancements in computational methods and probabilistic modelling have expanded the scope of TDR to include complex deterioration mechanisms such as carbonation, alkali-silica reaction, and fatigue [6, 9].

Live load models for bridge design are developed based on available truck surveys and other measurements. The maximum 50-75 year live load is determined through exponential extrapolation of the extreme values obtained from these surveys. Beam distribution factors are calculated using finite element analysis, and dynamic load is modeled using available test data. In the development of bridge design codes, the statistical parameters of live load are often assumed to be conservative, with truck traffic data taken from locations with a high volume of heavy vehicles [6, 10]. The novelty of our approach lies in the integration of time-dependent reliability into these load models. Unlike traditional methods, our procedure accounts for the increasing traffic load over time, which is critical for long-term durability design [6]. Research indicates that the mean load model is influenced by the load growth rate and the base period. The mean load is positively correlated with the base period, with this relationship becoming more significant as the load growth rate, denoted by q, increases [11]:

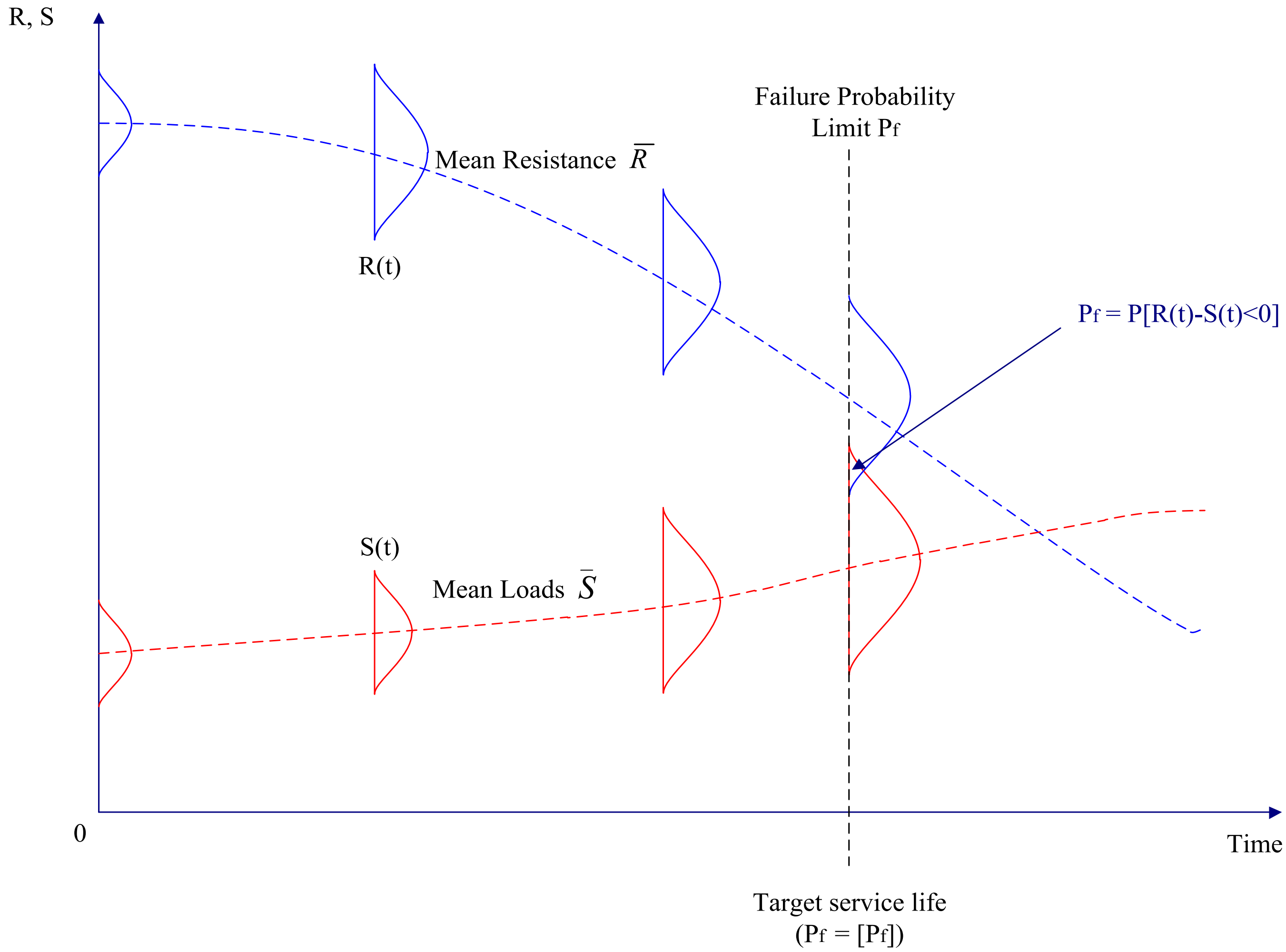

Fig. 1. Schematic representation of probabilistic service life design

$$n_{L(t)} = (1+q)^{t-1} \quad (1)$$

where $n_{L(t)}$ - traffic load increasing factor by time, which is $n_{L(t)} = \frac{\bar{L}_{(t)}}{\bar{L}_{(0)}}$.

Additionally, statistical analyses have shown that traffic load $\bar{L}_{(t)}$ increases linearly over time [12]:

$$\bar{L}_{(t)} = \bar{L}_{(0)}(1+q\cdot t) \quad (2)$$

where $\bar{L}_{(0)}$ - mean value of initial traffic load.

The bridge resistance degradation over time can be expressed as following formula [13, 14]:

$$R_{(t)} = R_{(0)} \cdot g_{(t)} \quad (3)$$

where $R_{(t)}$ - resistance dependent on time, $R_{(0)}$ - initial resistance, and $g_{(t)}$ is the resistance degradation function with a value range of [0,1] as following:

$$g_{(t)} = 1 - D_{(t)} \quad (4)$$

where $D_{(t)}$ -resistance deterioration over time.

The physical damage rate or resistance deterioration over time is expressed as follows [15]

$$D_{(t)} = e^{\lambda(t-T_0)} - 1 \quad (5)$$

where λ - the damage factor, which reflects the quality of the structures after manufacture and installation, the quality of the content according to the adopted operation strategy, the actual transport and natural and climatic conditions of the facility (average statistical value obtained for each element and span as a whole according to the results of the survey of more than 1000 Bridges) [15].

Recent research has demonstrated the potential of TDR to address the challenges of ageing bridges (Fig. 1). For instance, a novel procedure for durability design proposed and it integrates probabilistic models of material degradation and load variations [16]. The core concept of time-dependent reliability is schematically illustrated in Fig. 1. The figure depicts the fundamental interplay between structural resistance, $R_{(t)}$, and applied load, $S_{(t)}$, over time. The mean resistance, $\bar{R}$ typically degrades due to factors like corrosion and fatigue, while the mean load, $\bar{S}$ may increase due to growing traffic volumes. The probability of failure, P_f, is represented by the overlapping area of the two probability density functions at any given time, which increases as the distributions converge.

Reliability index β is generally used as a measure of reliability in EN 1990 (2002) and ISO 2394 (2015) [17, 18]. This index is related to failure probability through the inverse of the standardized normal cumulative distribution. Specifically, the reliability index (β) quantifies the number of standard deviations by which the mean resistance exceeds the mean load, providing a probabilistic measure of structural safety. The failure probability (P_f) is derived from the reliability index using the relationship $P_f = \Phi_{(-\beta)}$, where $\Phi_{(\cdot)}$ represents the standard normal cumulative distribution function. This inverse relationship underscores the importance of the reliability index in reliability-based design, as it directly links structural performance to probabilistic safety thresholds. For instance, a higher reliability index corresponds to a lower failure probability, ensuring a greater margin of safety [16]. This framework is particularly critical in time-dependent reliability analysis, where the degradation of resistance and increasing loads over time necessitate a dynamic assessment of failure probability throughout the structure's service life. The corresponding reliability index, $\beta_{(t)}$, shown in Fig. 2, decreases over the service life. This visualization underscores the limitation of static design codes and justifies the need for a time-variant reliability approach to accurately assess safety throughout a bridge's lifecycle.

The time-variant reliability index $\beta_{(t)}$ is derived from resistance $R_{(t)}$, dead load G, and live load $L_{(t)}$ (Formula (6) - (8)) [16]:

$$\beta_{(t)} = \frac{\bar{R}_{(t)} - \bar{L}_{(t)} - \bar{G}}{\sqrt{\sigma^2_{R_{(t)}} + \sigma^2_{L_{(t)}} + \sigma^2_{G}}} \geq \beta_{ULS} \quad (6)$$

$$\beta_{(t)} = \frac{\bar{R}_0 \cdot \bar{g}_{(t)} - \bar{L}_{(t)} - \bar{G}}{\sqrt{\bar{R}_0^2 \cdot \bar{g}^2_{(t)} \cdot (\nu^2_{R_0} + \nu^2_{g_{(t)}}) + \bar{L}^2_{(t)} \cdot \nu^2_L + \bar{G}^2 \cdot \nu^2_G}} \quad (7)$$

where β_{ULS} - Target reliability index for ULS, dependent on traffic load type (e.g., $\beta_{ULS(adjust)}$ = 2.95 for adjusted load, $\beta_{ULS(lim)}$ = 1.74 for increased load)

$\nu_{g(t)}$ - standard variation of resistance degradation at time t can be expressed as follows:

$$\nu_{g_{(t)}} = \frac{\bar{D}_{(t)}}{\bar{g}_{(t)}} \cdot \nu_{D_{(t)}} \quad (8)$$

$\nu_{D(t)}$- standard variation of resistance deterioration at time t.

Time-dependent reliability formulas transform static safety margins into adaptive metrics, harmonizing societal risk tolerance (via [P_{f1}]), operational dynamics (load-adjustment models), material physics (degradation laws).

The impact of train speed on dynamic loads is observed in various contexts. For instance, the dynamic load magnification factor for ballastless track-subgrades of high-speed railways largely depends on train speed [19]. Due to the complexity of vehicle-track-subgrade interaction, large-scale model tests are often employed to study these dynamic responses [19]. Likewise, the dynamic impact on bridge structures from high-speed trains moving at speeds from 100 km/h to 300 km/h has been studied [20]. For a comparative overview of alternative DIF formulations from several international codes, including those dependent solely on speed or incorporating track modulus and wheel diameter [21, 22, 23], see Table 1.

In this study, dynamic load management for railways is achieved through speed reduction, which directly controls the dynamic impact factor. We adopt the model, where the dynamic impact factor is given by DIF = (1+μ). This framework bridges theoretical rigor with practical constraints (e.g., speed limits), offering a living safety margin that evolves with the bridge's condition.

Their work highlighted the limitations of traditional design codes, which often fail to account for the time-dependent nature of bridge deterioration. By incorporating TDR into the design process, engineers can better predict the service life of ageing structures and optimize maintenance strategies.

Table 1. DIF formulations from literature

Source	DIF = (1 + μ)
AREMA [23]	$1+\frac{5.21\nu}{D}$
Clarke [21]	$1+\frac{19.65\nu}{D\sqrt{U}}$
Indian Railways [22]	$1+\frac{\nu}{58.14\sqrt{U}}$
South African Railways [21]	$1+\frac{4.92\nu}{D}$

μ is the dynamic increment coefficient, defined by the explicit speed-impact law, V is speed (km/h), D is the wheel diameter (mm), U is track modulus (MPa).

2.2. Performance - Based Durability Design

The application of advanced numerical simulations for bridge assessment is increasingly validated by field data. For instance, Nguyen et al. demonstrated the efficacy of combining Finite Element Method analysis with field measurements to accurately investigate cable tensions in cable-stayed bridges, showcasing a practical methodology for structural evaluation [24]. PBDD focuses on defining the required performance of a structure in terms of measurable criteria, such as load-carrying capacity, crack width, and deflection limits [16]. This approach allows for more flexible and adaptable design solutions, particularly for ageing bridges with complex deterioration patterns.

PBDD emerged as a response to the limitations of prescriptive design codes, which often fail to account for the unique challenges of each structure. Early applications of PBDD focused on high-performance concrete and advanced materials, where traditional specifications were inadequate [25]. In the context of bridge engineering, PBDD has been applied to optimize maintenance strategies and extend the service life of ageing structures [26].

Table 2. Classification of operating conditions of bridge components

#	Limit state	Measure	Reliability	Reliability index
1	Normal	-	0.999844	3.80
2	Restricted range of normal	Repair (no speed limit)	0.998363	2.95
3	Workable	Repair (speed limit possible)	0.992461	2.43
4	Restricted range of workable	Strengthening (transportation load and speed limit)	0.979771	2.05
5	Unworkable	Reconstruction or structural prohibition of traffic	0.958351	1.74(depends)

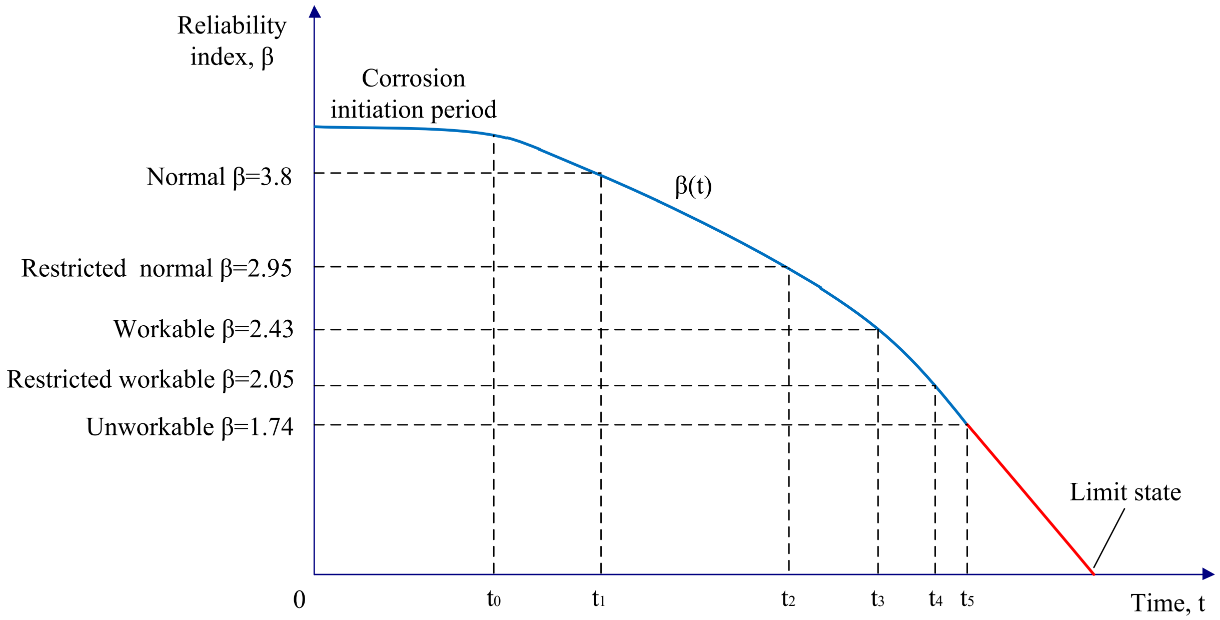

Fig. 2. Reliability for each DLS over time

The reliability indexes for each limit state of service life are suggested in [27, 28] are shown in Table 2 and Fig. 2.

Fig. 2 operationalizes the time-dependent reliability theory by mapping the decay of the reliability index $\beta_{(t)}$ against predefined performance thresholds. As $\beta_{(t)}$ declines from its initial value, it crosses thresholds that trigger specific operational states: from 'Normal' to 'Restricted,' 'Workable,' and finally 'Unworkable.'

These transitions, aligned with the limits states defined in Table 2, provide a clear, quantitative basis for maintenance decisions. For instance, when $\beta_{(t)}$ approaches the 'Restricted' threshold, it signals the need for repair interventions to restore safety margins. This figure is central to our proposed framework, as it translates abstract reliability calculations into actionable management strategies for bridge owners.

However, the application of PBDD remains limited due to the lack of standardized methodologies and practical guidelines. Current design codes often prescribe rigid material and process requirements, leaving little room for innovation or adaptation to modern materials and construction techniques [29]. This research aims to address this gap by developing a reliability-based design framework that integrates TDR and PBDD principles, providing a systematic approach to ensuring the long-term performance of ageing concrete bridges.

3. Methodology

This study proposes a novel, safety-first methodology for bridge failure prevention by integrating time-dependent reliability theory with dynamic load management strategies. The approach shifts from conventional static thresholds to a principled framework that optimizes real-time operational decisions (e.g., traffic/speed reduction) at ULS/SLS. Below, we outline the analytical framework, key solutions, and validation procedures.

3.1. Research Approach and Problem Formulation

This study proposes a safety-focused, time-dependent reliability framework to enhance bridge failure prevention, overcoming the limitations of conventional static reliability thresholds. By integrating dynamic load management with real-time operational adjustments, the methodology ensures structural safety while extending service life. Below, we outline the research's innovations, core challenges, and their mathematical formulations.

Traditional empirical or fixed-threshold methods are replaced with a dynamic model where reliability indices evolve over time. This accounts for material degradation (e.g., concrete corrosion, steel fatigue) and operational load variability. Proactive safety measures—such as reducing railway traffic speeds to 10–40 km/h—are triggered when β approaches critical thresholds (e.g., $\beta_{ULS} \approx 3.0$), balancing safety and functionality.

The framework dynamically modifies traffic loads to counteract reliability decay. For example, lowering dynamic impact factors through speed restrictions reduces effective loads, thereby delaying or maintaining compliance with ULS and SLS without premature bridge closures.

The key problems addressed are as following:

Time-Dependent Reliability Decay: Bridges initially designed with β values degrade due to environmental and operational stressors.

Minimum Safety Thresholds: Bridge operations must align with societally acceptable risk levels (e.g., 3×10^{-6} for motorcycles, 1.5×10^{-7} for aircraft, per J.P. Menzies' thresholds).

Post-repair, a bridge's load-carrying capacity ($L_{(t)}$) follows a sawtooth pattern:

Resistance Jumps: Post-repair capacity increases proportionally to investment (e.g., concrete reinforcement).

Decay Phase: Subsequent degradation is modeled using material durability equations, enabling predictive lifecycle management.

The framework synthesizes:

Time-Dependent Reliability Theory: $\beta_{(t)}$ formulations.

Operational Constraints: Context-dependent β values.

Real-Time Feedback: Adaptive load-resistance policies replace static thresholds.

By unifying dynamic reliability modeling, load management, and repair-impact analysis, this approach provides a scalable, safety-optimized solution for aging infrastructure, validated against empirical data and international standards.

3.2. Analytical Framework

The analytical framework underpinning this study synthesizes time-dependent reliability theory, dynamic load management, and repair-impact modelling into a cohesive system for bridge safety optimization. Unlike conventional static reliability thresholds, this framework treats reliability indices $\beta_{(t)}$ as dynamic variables, accounting for material degradation, operational load fluctuations, and proactive interventions. Below, we elaborate on its three core components: time-dependent reliability formulas, load adjustment strategies, and the impact of repair/reinforcement.

3.2.1. Time-Dependent Reliability Formulas

The core of bridge safety management lies in quantifying how structural reliability degrades over time due to material aging, environmental stressors, and operational loads. Unlike static reliability thresholds, time-dependent reliability models bridge failure probability as a dynamic function of exposure duration, load frequency, and resistance decay. This section elucidates the probabilistic framework, integrating societal risk thresholds, load-occurrence statistics, and adaptive safety margins.

Bridge failure probability P_f is decomposed into two interdependent factors:

Load occurrence probability (P_n): The likelihood of design loads (e.g., heavy freight trains) occurring within the last one year of the reference lifetime. For instance, Russian Code (1989) considers one time occurrence of design loads in the full reference lifetime (usually in the last one year), so P_n is modeled as [30]:

$$P_n = \frac{1}{365 \times 24 \times n_d} \quad (9)$$

where n_d is the frequency of critical loads per hour (e.g., n_d=3 for 72 train passages/day according to Russian Code [30]. This reflects the inverse relationship between load rarity and exposure time.

Conditional failure probability (P_{f1}): The failure likelihood given a load event, tied to the reliability index β. For a target β_{ULS} = 2.95, $P_{f1} \approx 1.6\times10^{-3}$ (from standard normal tables).

The total accident probability must satisfy:

$$P_f = P_n \cdot P_{f1} \le [P_{f1}] \cdot n_{f1} \quad (10)$$

where $[P_{f1}]$ is the societal tolerance (e.g., 3×10^{-6} for motorbike travel; from Menzies, [31]), and n_{f1} adjusts for exposure duration (e.g., 1/50 for railways with 1.2-minute train passages without train speed reduction vs. 1-hour reference).

Reliability index β is related to failure probability P_{f1} through the inverse of the standardized normal cumulative distribution. Specifically, the reliability index quantifies the number of standard deviations by which the mean resistance exceeds the mean load, providing a probabilistic measure of structural safety. The failure probability (P_{f1}) is derived from the reliability index using the relationship:

$P_{f1} = \Phi_{(-\beta)}$,

where $\Phi_{(\cdot)}$ represents the standard normal cumulative distribution function. This inverse relationship underscores the importance of the reliability index in reliability-based design, as it directly links structural performance to probabilistic safety thresholds. For instance, a higher reliability index corresponds to a lower failure probability, ensuring a greater margin of safety. This framework is particularly critical in time-dependent reliability analysis, where the degradation of resistance and increasing loads over time necessitate a dynamic assessment of failure probability throughout the structure's service life.

For instance, β = 3.78 aligns with airplane-level safety ($[P_{f1}]$ =1.5×10^{-7}), while β = 2.95 matches motorbike risks (Table 3). This ensures bridges operate within tolerable risk limits even as reliability decays.

Table 3. Societal risk thresholds and corresponding reliability indices for bridge design.

Risk Scenario	$[P_{f1}]$ (per hour)	Derived P_f	Target β
Motorbike travel	3×10^{-6}	0.0015768	2.95
Airplane/car travel	3×10^{-7}	0.00007884	3.78
Exceptional events	3×10^{-8}	0.000005256	4.41

The reliability index β decays nonlinearly due to:

Material degradation: Corrosion reduces steel cross-sections; concrete carbonation lowers strength.

Load accumulation: Traffic growth exacerbates fatigue damage.

A bridge's lifecycle is divided into two phases:

Phase 1 ($0 \le t \le T_1$): β decays from its initial value (e.g., β=4.2) toward ULS (e.g., β_{ULS} = 2.95). No interventions are needed unless β approaches the threshold.

Phase 2 ($T_1 \le t \le T_2$): Load reduction strategies (e.g., speed limits) activate to slow β decay or maintain β_{ULS} (e.g., β_{ULS} = 2.95). The dynamic impact factor $DIF_{(t)}$ decreases with speed, effectively lowering operational train loads. This extends service life until the minimum allowable load L_{lim} is reached, triggering SLS closure.

This study notes that fixed thresholds (e.g., β_{lim} = 1.74 for end-of-life) may misrepresent actual conditions.

Time-dependent reliability must reconcile with codified norms:

ISO 2394: Suggests β = 2.5–3.1 for ultimate states, but lacks time-variant guidance.

Ukrainian Codes: Stipulate β_n = 3.8 for "Normal" state and β_{ULS} = 2.95 for restricted operations [28].

Bridges may transition between standards-based β values as they age. For example, a bridge initially meeting $\beta_{(t<T1)}$ = 3.8 (airplane-level safety) might later operate at $\beta_{(T1)}$ = 2.95 (motorbike-level) with load restrictions.

3.2.2. Load Adjustment Strategies

The crux of this framework lies in its dynamic load management system, which proactively adjusts traffic demands to counteract reliability decay. Unlike static codes that mandate fixed load limits, this approach employs real-time feedback to balance safety and functionality.

Operational phases are divided into two phases:

Phase 1 ($0 \le t \le T_1$): Unrestricted Operations

Traffic loads increase per design projections, while material degradation gradually erodes resistance. Reliability decays passively until β approaches β_{ULS} (e.g., β_{ULS} = 2.95).

Phase 2 ($T_1 \le t \le T_2$): Adaptive Load Reduction

Upon reaching ULS, the system triggers load adjustments to maintain $\beta_{(t)} \ge \beta_{ULS}$. Key strategies include reducing speeds to 10–40 km/h decreases the dynamic impact factor $DIF_{(t)}$, effectively lowering the operational load spectrum for railway bridges, or restricting heavy vehicle access or enforcing lane reductions for highway bridges. The core concept is that all operational interventions—whether speed restrictions for railways or axle weight limits for highways—function by reducing the effective live load parameter in reliability calculations. The reliability index $\beta_{(t)}$ is then recomputed using the standard time-dependent reliability formulation with the adjusted live load parameters.

Based on the formulas of Kim et al., (2025), the formulas for approximated prediction of T_1 and T_2 are as following [16]:

Formulas (11), (12)

where $\nu_{g_{(t)}} = 0.15 \sim 0.3$ - standard variation of resistance degradation [16].

$$T_1 \approx T_0 + \frac{1}{\lambda} \cdot \ln[2 - \frac{\bar{G} \cdot (1 + 0.5625 \cdot \beta_{ULS} \cdot \nu_G) + \bar{L}_{(T_1)} \cdot (1 + 0.5625 \cdot \beta_{ULS} \cdot \nu_L)}{\bar{R}_0 \cdot [1 - 0.5625 \cdot \beta_{ULS} \cdot (\nu_{R_0} + \nu_{g_{(T1)}})]}] \quad (11)$$

$$T_2 \approx T_0 + \frac{1}{\lambda} \cdot \ln[2 - \frac{\bar{G} \cdot (1 + 0.5625 \cdot \beta_{ULS} \cdot \nu_G) + \bar{L}_{lim} \cdot (1 + 0.5625 \cdot \beta_{ULS} \cdot \nu_L)}{\bar{R}_0 \cdot [1 - 0.5625 \cdot \beta_{ULS} \cdot (\nu_{R_0} + \nu_{g_{(T2)}})]}] \quad (12)$$

The analysis reveals that relationships between all variables are nonlinear. Linearization methods—such as Taylor expansion (first-order approximation) for lifetime estimation—introduce significant approximation errors (up to 5 years). Therefore, the recommendation is to adopt a graphical method for higher accuracy. The simplified approach as formulas (11), (12) is reserved for design code applications only.

The time-dependent allowable live load $L_{adj(t)}$ is derived from resistance $R_{(t)}$ and target β (Formula (13)):

$$\bar{L}_{adj(t)} = \frac{\bar{R}_0 \cdot (1 - \bar{D}_{(t)}) \cdot [1 - 0.5625 \cdot \beta_{ULS} \cdot (\nu_{R_0} + \nu_{g_{(t)}})] - \bar{G} \cdot (1 + 0.5625 \cdot \beta_{ULS} \cdot \nu_G)}{1 + 0.5625 \cdot \beta_{ULS} \cdot \nu_L} \quad (13)$$

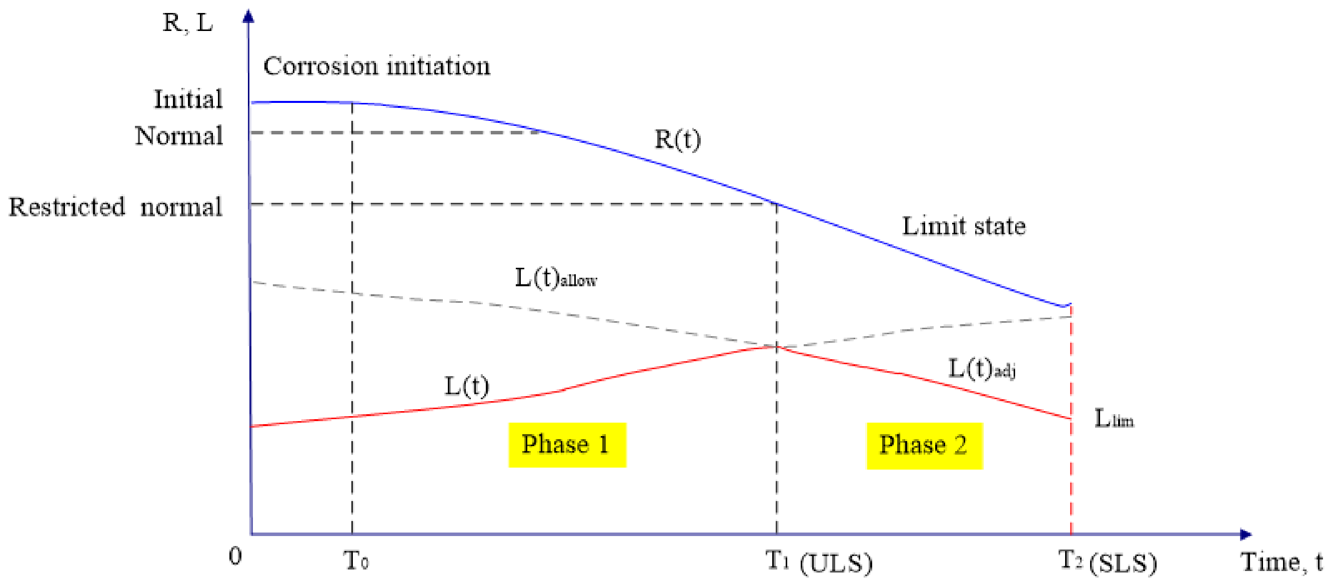

(a)

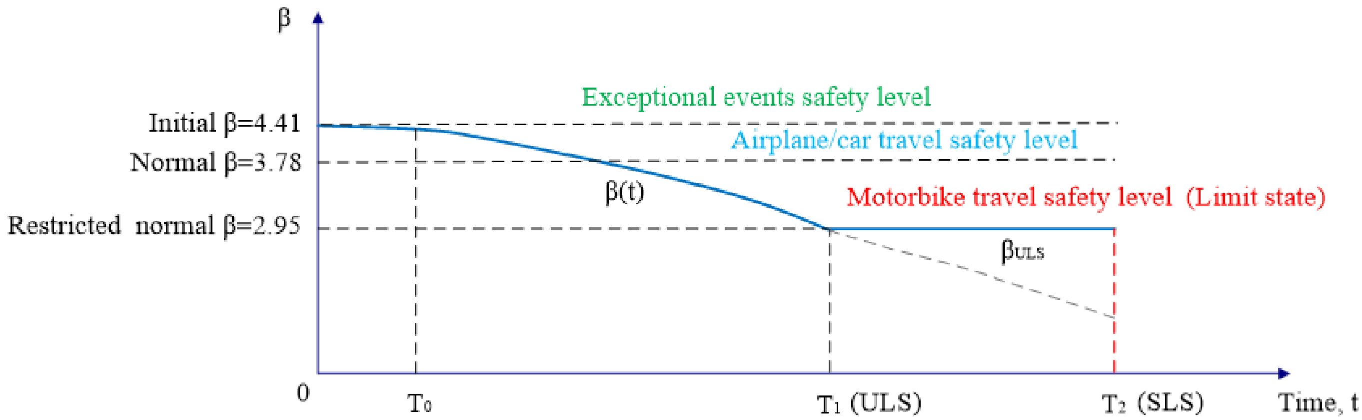

(b)

Fig. 3. Load-resistance equilibrium and reliability over a bridge's lifecycle:
a) Load-resistance equilibrium; b) Reliability (Phase 1 - Loads increase; resistance decays; Phase 2 - Loads decrease to stabilize β_{ULS})

This ensures β stabilizes near ULS until L_{lim} is reached (Fig. 3).

The step-by-step procedure of the proposed integrated framework is outlined in Fig. 3. The workflow begins with the input of initial bridge parameters, environmental data, and traffic models. It then proceeds to the core computational cycle: calculating the time-dependent reliability index $\beta_{(t)}$ at each time step by integrating probabilistic degradation models and load projections. The framework continuously checks $\beta_{(t)}$ against the performance limits from Fig. 2. If a threshold is breached, it triggers a specific output, such as a recommendation for load management or a detailed maintenance action. This flowchart provides a clear roadmap for implementing the framework in practice, ensuring all critical factors are considered systematically.

Practical Implications are as following:

Railway Bridges: Speed limits reduce dynamic forces, which dominate fatigue life.

Highway Bridges: Axle weight restrictions are more effective than traffic density controls for heavy freight routes.

This strategy transforms reliability management from a passive, code-compliant exercise into an active, data-driven process. By dynamically aligning loads with residual resistance, bridges achieve longer service lives without compromising safety—a paradigm shift from deterministic closures at arbitrary β thresholds.

3.2.3. Repair/Reinforcement Impact

The impact of repair or reinforcement on aging bridges is a cyclical process that temporarily restores structural capacity but does not halt the inevitable march of material degradation. Unlike static interventions prescribed by traditional codes, this framework treats repairs as dynamic "resets" within a bridge's lifecycle, where each intervention introduces a sawtooth-shaped recovery in load-carrying capacity. The essence lies in quantifying how these intermittent upgrades interact with time-dependent reliability decay—particularly in maintaining the ULS threshold ($\beta_{(t)} \geq \beta_{ULS}$) through adaptive load management.

a) The Sawtooth Trajectory of Post-Repair Resistance

When a bridge undergoes repair or reinforcement, its resistance $R_{(t)}$ experiences an immediate jump proportional to the intervention's scale. However, this recovery is transient. The renewed resistance immediately begins to decay again, influenced by the same environmental stressors that caused the initial deterioration. The decay rate post-repair may differ from the original trajectory if advanced materials or protective coatings are used, but the underlying physics of degradation remains unavoidable.

This cyclical pattern creates a sawtooth curve for $R_{(t)}$, where each repair episode postpones the bridge's eventual decline but does not eliminate it. The critical insight is that repairs are not a permanent solution but a tactical delay—a way to "buy time" until the next intervention or eventual replacement. The framework models this by integrating:

Step-function resistance jumps: $R_{(t)}$ increases discretely post-repair, with magnitude tied to investment.

Modified decay laws: Post-repair degradation may follow a gentler slope if superior materials are employed.

b) Dynamic Load Management after Repairs

Post-intervention, the bridge's operational load $L_{(t)}$ must be recalibrated to align with its restored capacity. Here, the framework diverges from conventional practice by treating load adjustments as a continuous feedback loop rather than a one-time recalculation. For instance, if a railway bridge's resistance improves after reinforcement, the permissible axle loads or train speeds might be increased temporarily. However, as $R_{(t)}$ decays anew, dynamic load restrictions (e.g., reducing speeds from 75 km/h to 25 km/h) are reactivated to maintain $\beta_{(t)} \geq \beta_{ULS}$.

This approach acknowledges a pragmatic reality: while repairs boost resistance, they rarely reset the clock entirely. For instance, a bridge repaired at year 30 might still reach ULS by year 40 (instead of year 35), but without load adjustments, it would breach safety thresholds sooner. The framework's innovation lies in synchronizing load management with repair cycles—ensuring that each intervention maximizes its residual life extension.

c) Economic-Safety Trade-offs and Predictive Lifecycle Modelling

The timing and scale of repairs are not just engineering decisions but economic ones. A minor patch-up might cost less upfront but necessitate more frequent interventions, while a comprehensive overhaul could defer the next repair for decades but strain budgets. The framework quantifies these trade-offs by linking investment levels to:

Resistance recovery: Higher investments yield larger $R_{(t)}$ jumps.

Decay rate modulation: Advanced techniques flatten the post-repair degradation curve.

Load adjustment flexibility: Bridges with higher post-repair resistance can tolerate heavier loads longer before restrictions are needed.

d) Harmonizing with Societal Risk Tolerance

Ultimately, repair strategies must align with the societal risk thresholds discussed earlier (e.g., β_{ULS} = 2.95 for motorbike-level safety). A bridge reinforced to β = 3.5 post-repair might initially permit unrestricted traffic, but as β decays toward β_{ULS} = 2.95, the framework enforces load limits to prevent breaching this red line. This dynamic balancing act ensures public safety while avoiding premature closures—a stark contrast to static codes that might mandate shutdowns at arbitrary resistance levels.

e) Conclusion: Repair as a Temporal Safeguard

The repair/reinforcement impact is not a one-time fix but a strategic pause in a bridge's reliability decay. By modelling interventions as periodic resets within a broader time-dependent framework, engineers can optimize both safety and service life. The key takeaway is that repairs gain true value only when integrated with real-time load management—a synergy that transforms static maintenance into a living, adaptive process.

3.3. Practical Implementation

The practical implementation of this methodology hinges on translating time-dependent reliability theory into actionable operational policies, ensuring bridges maintain safety thresholds through dynamic load adjustments. Here's how it unfolds in real-world scenarios.

a) Real-Time Load Prediction and Adjustment

Post-ULS, the framework shifts from passive monitoring to active intervention. Three load graphs guide decisions:

Planned Load Growth: Theoretical projections of traffic increases (pre-ULS).

Allowable Load Reduction: Safety-driven reductions post-ULS to stabilize $\beta_{(t)}$ near β_{ULS} by lowering dynamic impact factors—e.g., enforcing speed limits (10–40 km/h) for railway bridges or axle weight restrictions for highway bridges.

Composite Graph: The actual load trajectory, which follows Phase 1 until ULS is breached, then transitions to Phase 2's enforced reductions. This ensures operational loads never exceed the bridge's decaying capacity $R_{(t)}$ while avoiding premature closures.

b) Policy Integration

The framework replaces rigid safety margins with adaptive feedback loops tailored to each bridge's degradation rate and usage context:

Dynamic Compliance: Bridges transition between risk tiers (e.g., from β = 3.8 "Normal" state to β = 2.95 "Restricted" operations) as they age, aligning with societal risk tolerance. Regulatory bodies can adopt this phased approach to prioritize high-traffic routes for early interventions or staggered load limits.

Economic Optimization: By calibrating load reductions to $R_{(t)}$ decay—rather than arbitrary closure triggers—agencies defer costly replacements until the minimum allowable load L_{lim} is reached. For instance, a highway bridge might permit heavy trucks only during off-peak hours post-ULS rather than banning them outright.

In essence this validation marries theoretical rigor (ISO standards probabilistic foundations with pragmatic flexibility) bridge-specific adaptations. It proves that real-time reliability management isn't just academically sound, but operationally viable offering a blueprint for agencies grappling with aging infrastructure crises worldwide.

4. Results and Discussion

4.1. Case Study in the Previous Research

The foundational work by Kim et al. (2025) [16] provides a critical case study for this research, demonstrating the practical application of time-dependent reliability in durability design for reinforced concrete bridge beams. Their study addressed the limitations of static reliability indices by integrating probabilistic models of material degradation and traffic load variations. A key innovation was the introduction of a dynamic $\beta_{(t)}$ thresholding system, where reliability indices for ultimate limit states (β_{ULS}) and serviceability limit states (β_{SLS}) were calibrated to failure probabilities and functionally linked via load-reduction factors.

Here we discuss about the time-dependent factors such as reliability, resistance, load management (adjustment) and etc. based on as same case study as the 1-st case study of Kim et al., (2025) [16].

The application of the proposed framework to the case study bridge is presented in Fig. 4, which plots the calculated time-dependent reliability index $\beta_{(t)}$ under three phases: (1) a 'Do-Nothing' phase showing unchecked decay, (2) a phase with 'Dynamic Load Management' where traffic loads are adjusted as $\beta_{(t)}$ declines, and (3) a phase with 'Major Repair' at a specific intervention point. The results clearly demonstrate that the 'Do-Nothing' scenario leads to a rapid violation of the minimum safety threshold. In contrast, proactive load management effectively extends the service life by decelerating the reliability decay, while a major repair causes a sharp recovery of $\beta_{(t)}$. This figure validates the core advantage of our framework: enabling proactive, data-driven strategies to control the lifecycle safety of ageing bridges.

The time of corrosion initiation for edge and intermediate beams are 12.5years, 18.8years respectively.

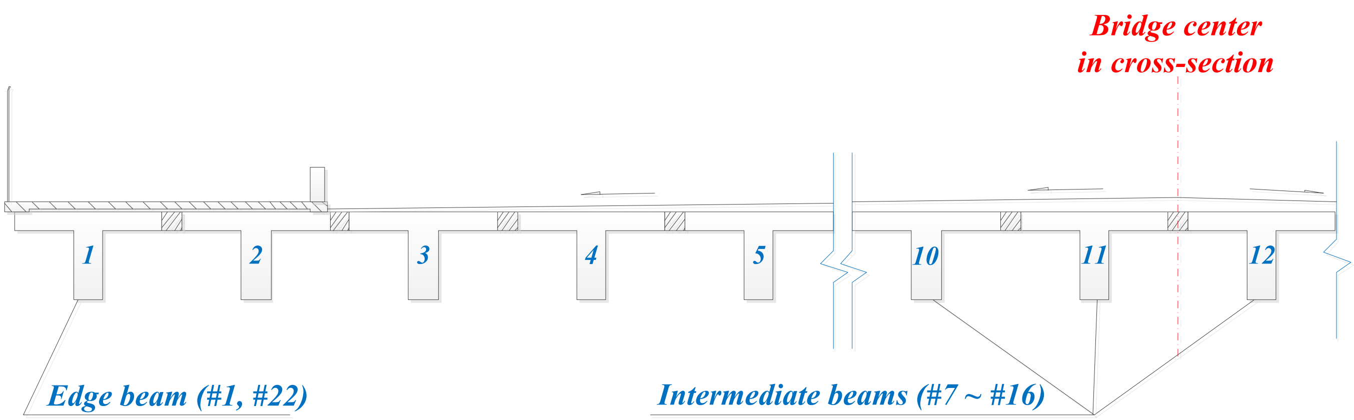

Fig. 4. Cross-sectional view of a reinforced concrete bridge with parallel beams.

According to the RC design code AASHTO, 2007, the resistance design equation is as follows (Eq. (14)):

$$1.0R_n = 1.25D_n + 1.75L_n \quad (14)$$

where $D_n = 1.0$, $L_n = 1.4$, $R_n = 3.7$.

The current load level is $L_0 = 1.1$ (i.e., the load growth rate is q=0.003). The basic data for reliability analysis was determined with reference to the literature [30, 32]. The statistical values for reliability evaluation are as follows (Table 4).

Table 4 Statistical data for resistance and loads

Resistance and loads	R	G	L
Mean	$1.2R_n = 4.44$	$1.05D_n = 1.05$	$0.5L_n$
COV	0.15	0.10	0.20

Traffic load growth is modeled non-linearly using Equation (1), reflecting realistic projections of increasing vehicular demands. This approach accounts for:

Exponential Extrapolation: Historical truck survey data are extrapolated to predict maximum live loads over 50–75 years (Eq. (1)).

$$\bar{L}_{(t)} = \bar{L}_{(0)} \cdot (1+q)^{t-1}$$

Dynamic Effects: Beam distribution factors and dynamic load amplification are derived from finite element simulations and field measurements.

These values capture inherent uncertainties in material strength, fabrication tolerances, and load variability, forming the basis for probabilistic reliability analysis.

The predicted service life T in the previous work corresponding to the reliability index $\beta_{ULS(lim)}$ = 1.74 was calculated as 43.7 years and 63.4 years respectively [16].

These findings reveal a critical limitation in current durability design practices: a fixed target reliability index fails to account for time-dependent variables during end-of-life deterioration, leading to two operational risks:

Inadequate safety margins: The reliability level may fall below motorcycle ULS standards (β_{ULS} = 2.95), creating hazardous conditions.

Uncertain load management: There is no systematic method to determine the exact load or speed reductions required to maintain safety during a bridge's final service stage.

This oversimplification stems from broader gaps in design codes:

Time-dependent reliability gaps: Static thresholds cannot model the dynamic interaction between progressive degradation and fluctuating traffic demands.

Code limitations: Current standards lack mechanisms to balance safety and live load adjustments during late-stage deterioration, as highlighted by Kim et al. (2025) [16].

4.2. Case Study: Novel Method for Dynamic Thresholding

This case study addresses the limitations of the previous approach by implementing a dynamic reliability threshold system, where the time-dependent reliability index $\beta_{(t)}$ governs actionable strategies for bridge management. The method operates in two distinct stages:

Stage 1 ($\beta_{(t)} \geq \beta_{ULS}$): Traffic growth is permitted until the bridge reaches its ULS at time TULS.

Stage 2 ($\beta_{(t)} = \beta_{ULS}$): Load restrictions (e.g., 50% axle weight limits) or speed reductions are enforced to mitigate dynamic impacts for railway bridges (e.g., reducing train speeds from 75 km/h to 25 km/h directly lowers the dynamic impact factor, DIF, which is calculated as (1+μ/3), by reducing the dynamic increment coefficient μ).

Key Findings from Calculations

For the edge and intermediate beams, the initial ULS thresholds (β_{ULS} = 2.95) were reached at T_1 = 30.2 years and T_1 = 45.6 years, respectively, based on prior results.

The highway bridge case assumes an 80-year reference lifetime with a load of 0.70. Adjusting axle weights to 50%, 60%, and 70% of the original limit (yielding 0.35, 0.42, and 0.49, respectively) allows calculation of the extended service lives T_2.

For β_{ULS}=2.52 and a 50% load limit

(L_{lim}=0.35), the predicted lifetimes T_2 were 40.0 years (edge beam) and 58.2 years (intermediate beam).

Comparative Analysis of Load Adjustments

In this study, the graphical method is employed for calculations, as detailed below.

The results, summarized in Table 5, reveal critical insights.

Fixed reliability thresholds fail to account for adjusted loads and actual reliability indices. For example, the default $\beta_{ULS(lim)}$ = 1.74 reflects only the design load, not real-world conditions.

At 50%, 60%, 70% load adjustments, $\beta_{ULS(lim)}$ exceeds 1.74, indicating higher risk compared to motorcycle trip safety benchmarks.

4.3. Case Study: Load Adjustment Strategies under Post-Repair Conditions

The preceding case study results indicate that the maximum service life of the edge beam without repair is 40 years when the traffic load is adjusted to 50% of the design load, while the intermediate beam achieves 56.2 years under a 60% load adjustment. Based on inspection and research findings, a repair strategy is proposed for the edge beam only.

The repair intervention improves the beam's resistance to 88.5% of its initial value (3.93 vs. 4.44) and delays corrosion initiation to 10 years (80% of the original initiation time). The post-repair deterioration process follows the same trajectory as before, but with the improved resistance and delayed corrosion initiation. This results in a net resistance gain of 0.9 (20.3% of initial resistance).

For the decade following repair (40–50 years), the resistance remains constant at 3.93. Beyond this period, deterioration resumes, mirroring the pre-repair trend. The resistance at year 50 is calculated as:

$R_{(50)} = R_{(40)} + 0.9 = 3.03 + 0.9 = 3.93$ (where $R_{(40)}$ = 3.03 from Table 5.

Table 6 presents the results of the authors' proposed framework for load adjustment and time-dependent reliability analysis.

Table 5. Load adjustment result for edge beam

Beam	T_1, year ($\beta_{(t)}$=2.95)	70% ($\beta_{(t)adj}$=2.95)		60% ($\beta_{(t)adj}$ =2.95)		50% ($\beta_{(t)adj}$ =2.95)		- % ($\beta_{(t)adj}$ = -)	
		T_2, year	$\beta_{ULS(lim)}$	T_2, year	$\beta_{ULS(lim)}$	T_2, year	$\beta_{ULS(lim)}$	T_2, year	$\beta_{ULS(lim)}$
Edge	30.2	35.8	2.59	37.2	2.44	40.0	2.29	44.8	1.74
Interm.	45.6	54.2	2.51	56.2	2.37	58.2	2.22	64.2	1.74

Table 6. Load adjustment strategies and reliability for edge beam over time

Time, year	Mean resistance	Mean dead load	Mean live load	Reliability by time	Mean allowable live load
t	Mean R	Mean G	Mean L	$\beta_{(t)}$	Mean $L_{(t)allow}$ (β_{ULS} = 2.95)
40 (before repair)	3.03	1.05	0.62	2.29	0.35 (50%)
40	3.93	1.05	0.62	2.97	0.73 (>100%)
45	3.93	1.05	0.63	2.95	0.73 (>100%)
50	3.93	1.05	0.64	2.95	0.73 (>100%)
55	3.63	1.05	0.65	2.40	0.42 (60%)
56.2	3.56	1.05	0.65	2.28	0.35 (50%)

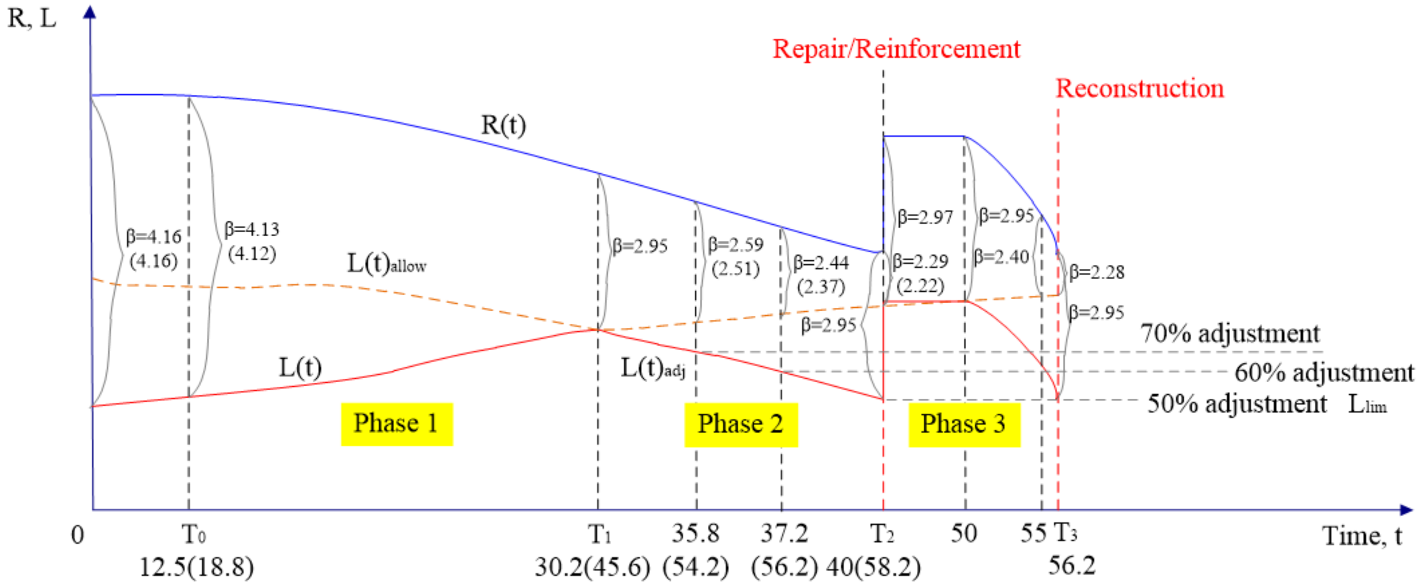

Fig. 5. Load adjustment strategies and reliability over a bridge's lifecycle for edge (intermediate) beams (Phase 1 - Loads increase; resistance decays; Phase 2 - Loads decrease to stabilize β_{ULS}; Phase 3 - Loads manage to stabilize β_{ULS} after repair)

A sensitivity analysis was conducted to identify the parameters with the greatest influence on the reliability index, and the results are shown in Fig. 5. The tornado diagram (or line plots) illustrates the impact of varying key inputs—such as the corrosion rate, initial traffic load, and load growth factor—on the calculated service life. The analysis reveals that the corrosion rate is the most sensitive parameter, indicating that the long-term safety of the bridge is highly dependent on the environmental conditions and material quality. This finding highlights the critical importance of accurate degradation models and suggests that investment in high-durability materials or protective coatings would yield the highest return in terms of lifespan extension.

Key Outcomes:

Traffic Load Capacity: Post-repair, the edge beam's live load capacity returns to 100% of the design load but gradually declines after corrosion reactivates, eventually stabilizing at 50%.

Service Life Extension: The repair delays the edge beam's failure from 40 to 56.2 years, aligning its lifespan with the intermediate beam.

Reliability Trends: As shown in Table 6, the reliability index peaks immediately after repair (2.97 at 40 years) and remains above the target (β_{ULS} =2.95) until year 50. By 56.2 years, $\beta_{(t)}$ drops to 2.28, necessitating load restrictions to 50%.

Implications:

Alignment of Lifespans: The repair (for only edge beams) harmonizes the service lives of both beams (56.2 and 58.2years, respectively), simplifying maintenance planning.

Dynamic Load Management: The study demonstrates the need for time-dependent load adjustments, with the edge beam transitioning from full capacity (40–50 years) to restricted loads (50–56.2 years).

Economic Efficiency: Targeted repair of the edge beam proves sufficient to extend the system's service life, avoiding costly full-span interventions.

This case study underscores the efficacy of integrating reliability-based repair strategies with dynamic load management, offering a scalable framework for ageing bridge maintenance.

5. Conclusion

This study successfully developed a reliability-based framework that integrates TDR with PBDD to address the challenges of ageing concrete bridges. The proposed methodology overcomes the limitations of traditional static design codes by dynamically modeling the interplay between resistance degradation and increasing traffic loads over time. A key innovation is the establishment of explicit links between time-variant reliability indices and actionable operational limits, providing a clear decision-making tool for bridge managers.

Case study applications demonstrated the practical utility of the framework, revealing that proactive load management strategies can effectively decelerate the decline in structural reliability, thereby extending service life without compromising safety. Furthermore, sensitivity analysis identified the corrosion rate as the most influential parameter on long-term performance, highlighting the critical importance of accurate degradation models and high-durability materials.

In summary, this research bridges a critical gap between theoretical reliability analysis and practical infrastructure management. The framework offers a rational, risk-informed approach for optimizing maintenance schedules, allocating resources efficiently, and ultimately enhancing the safety and longevity of our vital transportation assets. Future work will focus on automating the assessment process and integrating a broader range of complex, coupled deterioration mechanisms.

References

[1] G.M. Calvi, M. Moratti, N. Scattarreggia, V. Özsaraç, P.M. Calvi, R. Pinho. (2021). Numerical investigations on the collapse of the Morandi Bridge. Developments in International Bridge Engineering. *Springer Tracts on Transportation and Traffic, vol 17. Springer, Cham.* https://doi.org/10.1007/978-3-030-59169-4_1

[2] G. Santarsiero, A. Masi, V. Picciano, A. Digrisolo. (2021). The Italian guidelines on risk classification and management of bridges: Applications and remarks on large scale risk assessments. *Infrastructures,* 6(8), 111. https://doi.org/10.3390/infrastructures6080111

[3] G. Santarsiero, A. Masi, V. Picciano. (2021). Durability of Gerber saddles in RC bridges: Analyses and applications (Musmeci Bridge, Italy). *Infrastructures,* 6(2), 25. https://doi.org/10.3390/infrastructures6020025

[4] A. Mandić Ivanković, D. Skokandić, M. Kušter Marić, M. Srbić. (2021). Performance-based ranking of existing road bridges. *Applied Sciences,* 11(10), 4398. https://doi.org/10.3390/app11104398

[5] J. Rymsza. (2021). Causes of the collapse of the Polcevera Viaduct in Genoa, Italy. *Applied Sciences,* 11(17), 8098. https://doi.org/10.3390/app11178098

[6] Y. Liang, J.L. Yan, W.X. Qian, Z.Q. Cheng, H. Chen. (2021). Analysis of collapse resistance of offshore rigid frame-continuous girder bridge based on time-varying fragility. *Marine Structures,* 75, 102844. https://doi.org/10.1016/j.marstruc.2020.102844

[7] N. Galvão, J.C. Matos, D.V. Oliveira, R. Hajdin. (2022). Human error impact in structural safety of a reinforced concrete bridge. *Structure and Infrastructure Engineering,* 18(6), 836-850. https://doi.org/10.1080/15732479.2021.1876105

[8] L.S. Ho, H.T.T. Ngo, H.T. Vu, , S.T. Nguyen, V.N. Chau, V.Q. Dang. (2023). Durability of mortar and concrete containing pozzolans as a partial cement replacement in the marine environment: A review. *Journal of Science and Transport Technology,* 3(3), 13-25. https://doi.org/10.58845/jstt.utt.2023.en.3.3.13-25

[9] F. Biondini, D.M. Frangopol. (2016). Life-cycle performance of deteriorating structural systems under uncertainty: Review. *Journal of Structural Engineering,* 142(9), F4016001. https://doi.org/10.1061/(ASCE)ST.1943-541X.0001544

[10] A.S. Nowak, M.M. Szerszen. (2000). Structural reliability as applied to highway bridges. *Progress in Structural Engineering and Materials,* 2(2), 218-224.

https://doi.org/10.1002/1528-2716(200004/06)2:2%3C218::AID-PSE27%3E3.0.CO;2-8

[11] W. Xu, Y. Qian, C. Jin, W. Gong. (2024). An improved time-dependent reliability model for aging RC bridges based on GPD load distribution. *KSCE Journal of Civil Engineering,* 28(6), 2245-2256. https://doi.org/10.1007/s12205-024-1902-x

[12] V.A. Ilich, V.S. Nazaralievich, S.V. Sergeevich, O.I. Georgievich. (2022). Long-term degradation processes affecting the reduction of load capacity and durability of bridge structures during their maintenance (in Russian). *The Eurasian Scientific Journal,* 14(2), 55SAVN222.

[13] M.P. Enright, D.M. Frangopol. (1998). Probabilistic analysis of resistance degradation of reinforced concrete bridge beams under corrosion. *Engineering Structures,* 20(11), 960-971. https://doi.org/10.1016/S0141-0296(97)00190-9

[14] Y. Mori, B.R. Ellingwood. (1993). Reliability-based service-life assessment of aging concrete structures. *Journal of Structural Engineering,* 119(5), 1600-1621. https://doi.org/10.1061/(ASCE)0733-9445(1993)119:5(1600)

[15] A.I. Vasilyev. (2020). Degradation processes and residual resource durability of bridge elements (in Russian). *Automobile, Road, Infrastructure,* 1(23), 1-15.

[16] Y. Kim, X. Mi, M. Yang, C. Ri, M. Chen. (2025). Durability design of reinforced concrete bridges using time-dependent reliability. *Proceedings of the Institution of Civil Engineers – Bridge Engineering,* 178(3). https://doi.org/10.1680/jbren.25.00002

[17] CEN. (2002). EN 1990: Eurocode – Basis of structural design. Brussels: CEN.

[18] ISO. (2015). ISO 2394: General principles on reliability for structures (4th ed.). Geneva: ISO.

[19] R. Chen, X. Zhao, Z. Wang, H. Jiang, X. Bian. (2013). Experimental study on dynamic load magnification factor for ballastless track-subgrade of high-speed railway. *Journal of Rock Mechanics and Geotechnical Engineering,* 5(4), 306-311. https://doi.org/10.1016/j.jrmge.2013.04.004

[20] H. Siguerdjidjene, L.K. Dyachenko. (2021). Study of dynamic impact of speed trains on bridge structures. *International Journal of Mechanics,* 15, 30-36. https://doi.org/10.46300/9104.2021.15.4

[21] N.F. Doyle. (1980). Railway track design: A review of current practice. *Bureau of Transport Economics.*

[22] M. Srinivasan. (1969). Modern permanent way. *Somaiya Publications*.

[23] W.W. Hay. (1982). Railroad engineering (Vol. 1). *John Wiley & Sons*.

[24] D.T.T.D. Nguyen, T.N. Nguyen, A. Saleem, J.H. Park, H. Ho. (2025). Investigation of cable tension in cable-stayed bridges through field measurements and numerical simulation. *Journal of Science and Transport Technology,* 5(2), 71-83. https://doi.org/10.58845/jstt.utt.2025.en.5.2.71-83

[25] E.C. Bentz. (2000). Life-365 service life prediction model. *Concrete International,* 22(5), 53-58.

[26] D.M. Frangopol, M. Liu. (2007). Maintenance and management of civil infrastructure based on condition, safety, optimization, and life-cycle cost. *Structure and Infrastructure Engineering,* 3(1), 29-41. https://doi.org/10.1080/15732470500253164

[27] D.A. Shestovitskiy. (2021). Justification of reliability and service life of designed bridges (in Ukrainian). *Bridges and Tunnels: Theory, Research, Practice*. UDC 624.21.093.004

[28] Ministry of Regional Development and Construction of Ukraine. (2009). DSTU-N BV.2.3-23:2009. Guidelines for assessing and predicting the technical condition of highway

bridges.

[29] American Concrete Institute. (2000). ACI Committee 365. Service-life prediction—State-of-the-art report.

[30] Bondarovich BA, Potapkin AA, Tserbakov EN et al. (1989). Recommendations for assessing and ensuring the reliability of transport structures. (in Russian). https://snip.ruscable.ru/Index1/41/41950.htm

[31] M. Lemaire. (2009). Structural reliability. *Spon Press. ISTE, John Wiley & Sons,* ISBN: 978-1-84821-082-0.

[32] C. Wang, Q. Li, A. Zou, L. Zhang. (2015). A realistic resistance deterioration model for time-dependent reliability analysis of aging bridges. *Journal of Zhejiang University-SCIENCE A*, 16, 513-524. https://doi.org/10.1631/jzus.A1500018